



DETECT: seismological data from multiple dense arrays deployed across the Irpinia fault system in southern Italy

Francesco Scotto di Uccio¹, Angelo Strollo², Matteo Picozzi^{1,9}, Dino Bindi², Antonio Scala¹, Gaetano Festa¹, Tony Alfredo Stabile³, Erwan Gueguen³, Guido Maria Adinolfi^{4,12}, Claudi Martino⁵, Ortensia Amoroso⁷, Raffaella De Matteis⁴, Vincenzo Convertito⁵, Daniele Spallarossa⁷, Alessandro Caruso², Francesco Carotenuto¹, Simona Colombelli¹, Grazia De Landro¹, Gregory De Martino³, Luca Elia¹, Benjamin Heit², Laure Hillmann², Antonio Giovanni Iaccarino¹, Mauro Palo¹, Karina Loviknes², Stefan Mroczek², Sahar Nazeri¹, Titouan Muzellec¹, Ferdinando Napolitano⁶, Serena Panebianco³, Raffaele Rea¹, Rosario Riccio⁵, Guido Russo¹, Vincenzo Serlenga³, Stefania Tarantino^{1,10}, Nicola Tragni^{3,11}, Thomas Zieke², Jannes Münchmeyer², Peter Makus², Alister Trabattoni⁸, Aldo Zollo¹, Fabrice Cotton²

¹ Università degli studi di Napoli Federico II - Dipartimento di Fisica "Ettore Pancini", 80126, Napoli, Italy

² GFZ Helmholtz Centre for Geosciences, Potsdam, 14169, Germany (ROR ID <https://ror.org/04z8jg394>)

³ CNR - Institute of Methodologies for Environmental Analysis, Italy

⁴ Università degli Studi del Sannio, Dipartimento di Scienze e Tecnologie, Benevento, Italy

⁵ Istituto Nazionale di Geofisica e Vulcanologia - Osservatorio Vesuviano, Italy

⁶ University of Salerno, Italy

⁷ University of Genoa, Italy

⁸ École Supérieure d'Électronique de l'Ouest (ESEO), Angers, France

⁹ National Institute of Oceanography and Applied Geophysics – OGS, Trieste, Italy

¹⁰ Now at Istituto Nazionale di Geofisica e Vulcanologia - L'Aquila, Italy

¹¹ Now at Italferr S.p.A., Italy

¹² Now at Università di Torino, Dipartimento di Scienze della Terra, Turin, Italy

Correspondence to: Francesco Scotto di Uccio (francesco.scottodiuccio@unina.it)

Abstract:

We present a large seismological dataset (<https://geofon.gfz.de/doi/network/ZK/2021>) composed by continuous recordings from 200 temporary stations (seismic network ZK, 10.14470/MX7576871994), which operated continuously for approximately one year in the Southern Apennines (Southern Italy) as part of the DETECT experiment. The dataset is compliant with the seismological standards for the archiving of data and metadata, and with standardized tools for disseminating them, e.g., the International Federation of Digital Seismograph Networks (FDSN) web services. The data set was collected during the DETECT experiment in the Irpinia area (southern Italy), which is one of the regions with the highest seismic hazard in Italy. From August 2021 to August 2022, a constellation of 20 seismic arrays, with a total of 200 seismic stations, was installed above the fault segments responsible for the M 6.9, 1980 Irpinia earthquake, the strongest and most destructive seismic event in Italy in the last fifty years. Each seismic array had a maximum aperture of ~2 km and was composed of one broad-band sensor,



38 one short-period sensor with 1 Hz and eight 4.5 Hz natural frequency geophones. Data and metadata were managed
39 in accordance with the GIPP/GEOFON policy using SeisComp (Helmholtz Centre Potsdam – GFZ German
40 Research Centre for Geosciences and GEMPA GmbH, 2008) and the final archive size is approximately 5.2 TB.
41 In this contribution, we provide details on how to download waveform data and station metadata, as well as
42 information on data availability and quality.
43

44 1. Introduction

45 Italy is one of the most seismically hazardous country in Europe, with the strongest historical earthquakes all
46 characterized by magnitudes between 6 and 7 (i.e., the 1857 Mw 7.0 Basilicata earthquake, the 1908 Mw 7.0
47 Messina earthquake, the 1915 Mw 6.7 Fucino earthquake, the 1976 Mw 6.5 Friuli earthquake, the 1980 Ms 6.9
48 Irpinia earthquake, the 2009 Mw 6.3 L’Aquila earthquake, and the 2016 Mw 6.5 Norcia earthquake; Rovida et al.,
49 2020). Despite their moderate magnitudes, the combination of elevated seismic hazard and high structural
50 vulnerability places communities and infrastructures in significant danger from earthquakes.

51 In the context of seismic risk mitigation actions, scientists are deeply involved in improving the understanding of
52 how seismic sequences evolve and the preparatory phase preceding major earthquakes. To this end, characterizing
53 the spatio-temporal distribution and source properties of microearthquakes is a mean to shed light on stress
54 accumulation and fault weakening processes that may anticipate a large rupture (Picozzi et al., 2022a). Furthermore,
55 microearthquakes also help to monitor changes in the medium’s elastic properties (Di Luccio et al., 2010, Adil et
56 al., 2025) and can support the management of industrial activities in the context of anthropogenic seismicity (Stabile
57 et al., 2021). For these reasons, in recent years, temporary dense arrays have been installed to enable high-resolution
58 seismic imaging and monitoring, and to advance understanding of the dynamics of fault zones (Ben-Zion et al.,
59 2015; Gradon et al., 2020).

60 This work presents and opens to the community the dataset acquired during an innovative monitoring experiment
61 carried out in the Irpinia fault system in the southern Apennines, Italy, named “Dense mulTi-paramEtriC
62 observations and 4D high resoluTion imaging”, or DETECT (Bindi et al., 2021). The DETECT target area was
63 struck by the 23 November 1980, Ms 6.9 Irpinia earthquake, which occurred along NW-SE striking faults. It was
64 characterized by three main episodes that occurred within seconds of each other, resulting in approximately 3,000
65 fatalities and widespread damage (Bernard & Zollo, 1989). The network code assigned by the International
66 Federation of Digital Seismograph Networks (FDSN) is ZK (doi: [10.14470/MX7576871994](https://doi.org/10.14470/MX7576871994)). The continuous
67 waveform archive is entirely stored in the European Integrated Data Archive (Strollo et al., 2021) and is made
68 available via standard FDSN-compliant web services (Bindi et al., 2021). For more information, please refer to the
69 Data availability section.

70 The DETECT experiment had two main objectives: 1) investigating technological solutions to enhance seismic
71 monitoring capabilities and 2) improving our understanding of the temporal and spatial evolution of seismicity and
72 its relationship with crustal fluids. The experiment involved the deployment of a dense network of around 200
73 seismic stations along the Irpinia fault system over a period of one year. These stations were organized into seismic
74 arrays that demonstrated a high potential for detecting and locating natural and anthropogenic seismic sources (Rost

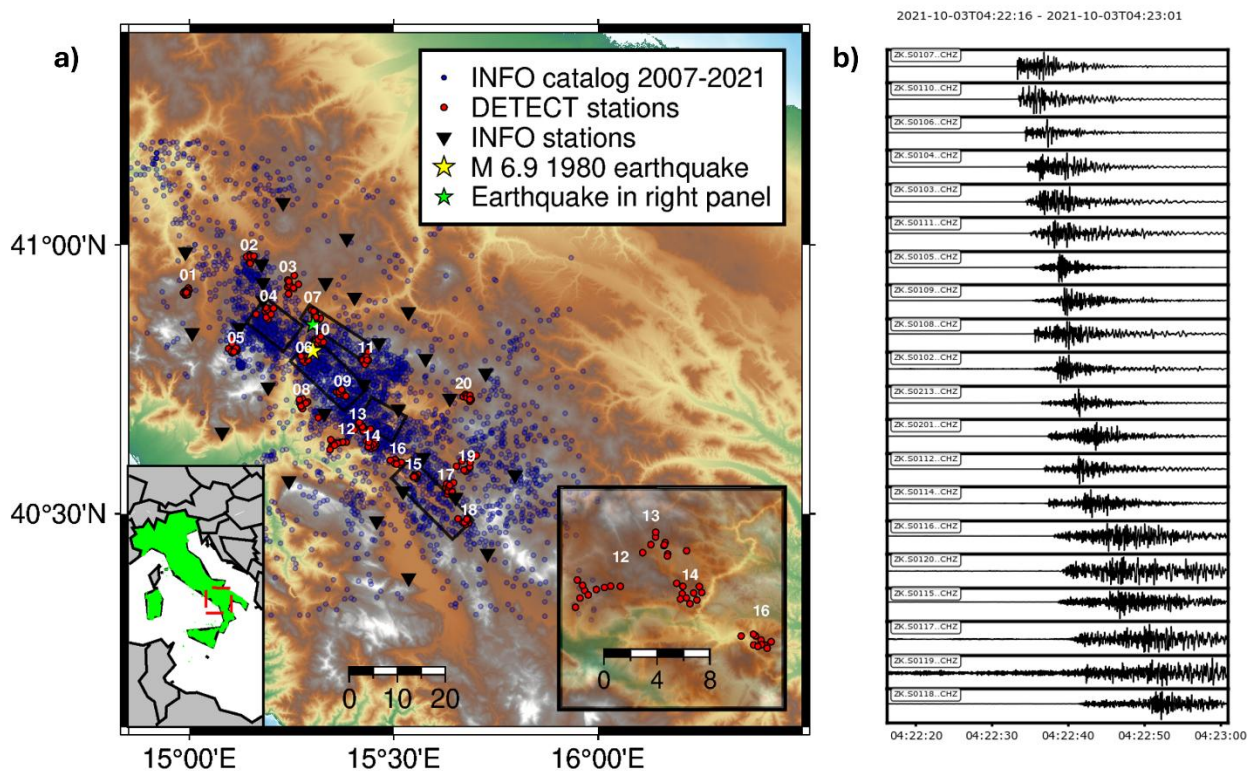


75 & Thomas, 2009; Picozzi et al., 2011). Consequently, the DETECT dataset presented in this study can provide
76 unique imaging and tracking of crustal fluids by lowering the detection threshold of the Irpinia Near Fault
77 Observatory (INFO, <https://www.epos-eu.org/tcs/near-fault-observatories>; Chiaraluce et al., 2022), which has been
78 monitoring seismic activity in the area since 2005.

79 This manuscript details the technical aspects of the DETECT experiment, including network design, station
80 deployment, and operational procedures, together with the data processing steps for format conversion and quality
81 control. Besides sharing the waveforms collected during the one-year experiment, we also introduce and share with
82 the community the enhanced catalog of microseismic events obtained by applying advanced detection strategies to
83 the presented DETECT dataset (Scotto di Uccio et al., 2026). The resulting dataset holds promise for developing
84 and testing monitoring methodologies aimed at: (1) recognizing evolving spatiotemporal trends in source
85 parameters that may imply large-earthquake nucleation; (2) examining the frictional and stress states of fault
86 segments in order to forecast future seismic energy release; and (3) evaluating the interactions among fault
87 segments to better understand and potentially anticipate cascade failure mechanisms.

88 **2. The DETECT target region**

89 The tectonics of the Irpinia region is now dominated by active, extensional faults arranged in subparallel structures,
90 mainly disseminated over the Apennines axial sector, with trends mainly ranging from WNW-ESE to NW-SE
91 (Adinolfi et al., 2019; Bello et al., 2021). Since 2005, the Irpinia Near Fault Observatory (INFO) has been
92 monitoring seismic activity in the area. INFO includes the Irpinia Seismic Network (ISNet;
93 <https://isnet.fisica.unina.it>; Iannaccone et al., 2010), which comprises 31 seismic stations (black triangles in Figure
94 1).
95



96
97
98 **Figure 1. a)** Map with all DETECT stations (red circles) with Array ID (name of hosting municipality is given in Table 2), blue circles are
99 indicating all events recorded by the INFO network (stations indicated with black triangles) from 2007 to 2021, black rectangles indicating
100 the different fault segments (DISS Working Group, 2025) of the Ms 6.9 1980 Irpinia Earthquake (yellow star). The green star indicates the
101 actual location of the M2.3 of 2021-10-03 event, recorded at all DETECT stations. The right-side inset highlights some examples of different
102 array geometries for arrays 12, 13, 14 and 16 **b)** Vertical component of velocimetric records at the broadband stations for the M2.3 earthquake
103 in the panel (a).
104

105 As recorded by ISNet, the seismicity appears distributed in an area of approximately 3,700 km² (ca. 80 km × 46
106 km). The largest recent events ranged from Mw 3.4 in 2009 to Mw 4.1 in 2025. The hypocenters of the present-day
107 earthquakes appear to be spread over a large crustal volume around the fault segments that generated the Ms
108 6.9 Irpinia earthquake (yellow star in Figure 1). These earthquakes span depths from 2 to 20 km, with a higher
109 density of events between 7 km and 12 km in carbonate lithology. Therefore, the seismically active rock volume
110 consists of the Apulian Platform carbonates and their basement. Occasionally, the seismicity in the area occurs as
111 seismic sequences originating on structures oriented as the larger faults that generated the 1980 Irpinia earthquake
112 (Stabile et al., 2012; Festa et al., 2021; Scotto di Uccio et al., 2024). These sequences in Irpinia appear either to
113 occur on subparallel, smaller-scale faults or to rupture patch-wise on the main faults in segments that were locked
114 during previous events (Palo et al., 2023; Scotto di Uccio et al., 2024).

115 Notably, this sector of the southern Apennines, which is far from active volcanism (>70 km), is characterized by
116 the remarkable outgassing of deep-origin volatiles, with carbon dioxide (CO₂) being the dominant gaseous species
117 (Improta et al., 2014; Caracausi et al., 2022). Crustal fluids have been shown to play an active role in regional



118 seismicity (Chiodini et al., 2004). In Irpinia, the background microseismicity and seismic sequences appear to be
119 partially controlled by fluids of different origins (Amoroso et al., 2014; D’Agostino et al., 2018; Tarantino et al.,
120 2024).
121 Recent studies that exploited the long-term monitoring of the microseismicity provided evidence of structural
122 segmentation and insight into the evolution of both crustal and source properties, inferred from the medium
123 properties (eg., De Landro et al., 2022), the apparent stress (Picozzi et al., 2019), the stress drop (Picozzi et al.,
124 2022b) and the ground motion intensity (Picozzi et al., 2022c).

125 3. Network design, deployment, and operation

126 DETECT was conceived using limited household funding from the University of Napoli Federico II (UniNA) and
127 the Helmholtz Centre for Geosciences (GFZ), without additional third-party funding. The project leveraged the
128 personnel and logistical resources available at all partner institutions. Despite the limited budget, the survey was
129 designed to capture small events while integrating the coverage of the standard network. Building on the success
130 of previous experiments in monitoring microseismicity and seismic tremor with small-scale arrays (Scala et al.,
131 2022; Panebianco et al., 2024), we deployed 200 seismic stations in 20 arrays, each consisting of ten stations (Table
132 1 and 2, red dots in Figure 1). The Geophysical Instrument Pool Potsdam (GIPP, <https://www.gfz.de/gipp>) provided
133 the seismic equipment for DETECT, and GFZ and UniNA provided all other necessary accessories to operate the
134 stations. The first pilot array (ID 08, Table 2) was deployed in the epicentral area of the 1980 Ms 6.9 Irpinia
135 earthquake in June 2021, with an initial sampling rate of 400 Hz. After preliminary analyses evaluating costs and
136 benefits, the sampling rate was reduced to 200 Hz for the entire experiment.

137 During the preparation phase of the deployment, the municipality of Colliano (SA) organized and hosted an
138 outreach event, in which researchers participating in the campaign presented the aims of the experiment to the
139 mayors of other municipalities later involved in DETECT. This raised awareness among the local administrations,
140 all of which supported the deployment of all the other arrays (Table 2). The arrays were installed between late
141 August and late September 2021 by small crews (four crews of two to three people). The arrays were located in
142 small municipalities in Irpinia for two reasons: i) the local authorities and citizens were available to host the seismic
143 stations, helping with scouting and guaranteeing the security of the sites while allowing to disseminate knowledge
144 about hazard and seismicity of the area; ii) the arrays were installed as close as possible to the fault segments
145 involved in the 1980, Ms 6.9 Irpinia earthquake (Figure 1).

146 Consequently, the arrays had variable geometry optimized for the local conditions (dynamic map at
147 <https://geofon.gfz.de/waveform/archive/network.php?ncode=ZK&year=2021>, and inset in Figure 1), and an
148 approximate aperture size of 2 km. This size was envisaged based on the findings of De Landro et al. (2020), who
149 assessed the potential of including similar arrays in monitoring systems for induced seismicity. They found that,
150 for low noise levels, integrating seismic networks with small-scale arrays can achieve a magnitude detection
151 threshold close to Mw 0 and small location errors (i.e., a few hundred meters for depths down to 8 km).

152 All the stations were equipped with CUBE 3 Digital recorders, and each array consisted of nine short-period sensors
153 (eight 4.5 Hz Geophone 3-C and one Mark L-4C 3D 1Hz Geophone 3-C) and one broadband seismometer (Trillium
154 Compact 120). The right panel of Figure 1 shows the vertical component of the ground motion records of the
155 broadband sensors for a M2.3 earthquake (green star). When possible, broadband stations were installed at sites
156 with power supply or powered by solar panels. All the other stations were powered by 9V/200 Ah or 9V/175Ah
157 dry, super alkaline batteries. When possible, the sensors were installed in small holes and covered with a plastic
158 crate, also containing the data logger and the battery (Figure 2).



159
 160

Instrument type	Name	Manufacturer	Units used	Link to GIPP Instrument data base
Digital recorder	CUBE 3 ext	Omnirecs/DIGOS	20	https://gipp.gfz.de/instrumentcategories/view/29
Digital recorder	CUBE 3 int	Omnirecs/DIGOS	180	https://gipp.gfz.de/instrumentcategories/view/28
Seismic sensor	Trillium Compact 120	Nanometrics	20	https://gipp.gfz.de/instrumentcategories/view/15
Seismic sensor	Mark L-4C-3D 1Hz Geophone 3-C	Sercel	20	https://gipp.gfz.de/instrumentcategories/view/4
Seismic sensor	4.5Hz Geophone 3-C	Sensor Netherland	160	https://gipp.gfz.de/instrumentcategories/view/5

161
 162
 163
 164
 165
 166

Table 1. Instruments used for the DETECT experiment as provided by GIPP (Grant Number 202119). Instrument (sensor) type information is also embedded in the second and third characters of the station codes: 01 for Trillium Compact 120, 02 for Mark L-4C-3D 1 Hz Geophone 3-C and 03-10 for 4.5 Hz Geophone 3-C (only 2 stations are not following this convention S0203 and S1003 at Array #03, where the two sensors were swapped).

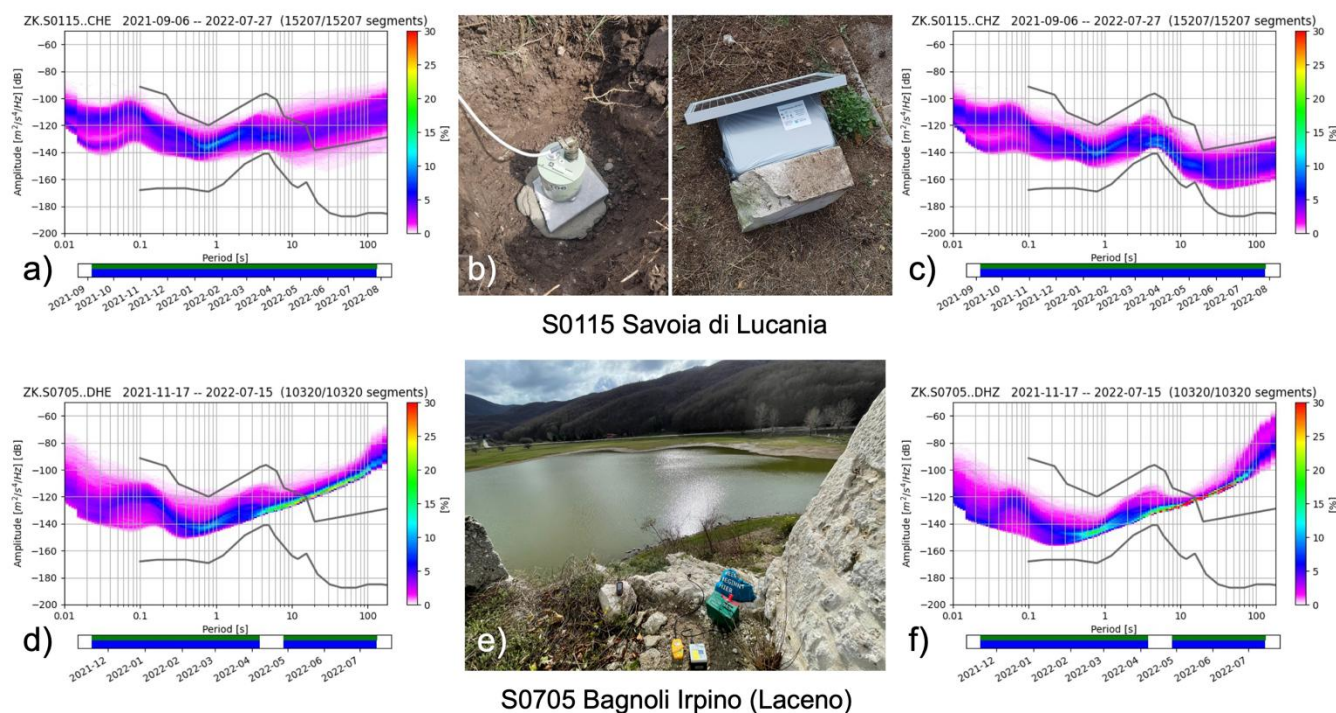


Figure 2. Probability Density Functions (PDFs) computed for two example stations: upper panels for Savoia di Lucania, Array ID 15, station S01 equipped with Broad-Band sensor Trillium Compact 120, a) East component, b) picture of the installation, c) vertical component, lower panels for Bagnoli Iripino (Laceno) Array ID 05, station S07 4.5 Hz Geophone 3-C (Table 2), d) East component, e) picture of the installation, f) vertical component.

To limit power consumption, the experiment was realized without real-time data transmission. This required periodic visits to each station to download the acquired data.

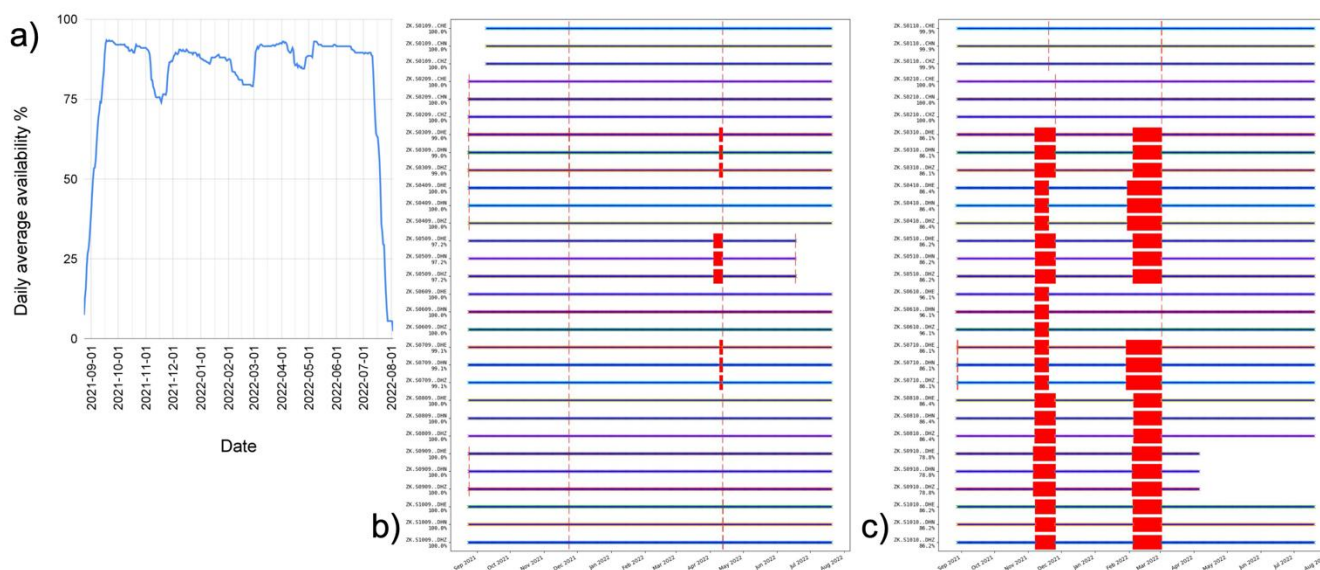
The complete list of installed instruments (DETECT metadata) is available in both *text* and *station_xml* formats in various levels of resolution (station, channel, response) from the GEOFON data center (see the Data Availability section). The installation and data curation followed the guidelines by Heit et al. (2021) for a large number of stations, as in the Alps.

4 Data collection and curation

The crews visited the seismic stations three times (November–December 2021, March–April 2022, and July–August 2022) to retrieve data and replace batteries. During each visit, data were transferred from the dataloggers onto external storage devices and subsequently transferred to GEOFON for further processing. We collected 4.5 TB of data during the first recovery campaign, 4.3 TB during the second one, and 4.0 TB during the final campaign. The overall data availability for the period from 21 October 2021 to 11 July 2022 was 88%. Data availability remained generally stable over time, except for short intervals preceding maintenance visits, when it temporarily



187 decreased to 75–80% due to internal storage saturation or battery depletion (Figure 3a). Since individual arrays
188 were installed within a few days, storage saturation issues occurred almost simultaneously at all stations of a single
189 array (Figure 3b-c).



190
191 **Figure 3.** a) Overall daily average data availability for the entire network. b) and c) Station availability over the entire time span for two
192 arrays, respectively 09 and 10 (Table 2).
193

194 To optimize the maintenance schedule, a traffic-light system was implemented within a webGIS platform, available
195 throughout the experiment, indicating the time elapsed since the last data download for each station. This system
196 enables efficient prioritization of field activities and route planning, resulting in significant savings in time and
197 resources. In addition, a Telegram bot was developed to streamline communication and updates, while QR codes
198 installed at each station facilitate rapid identification and interaction in the field.

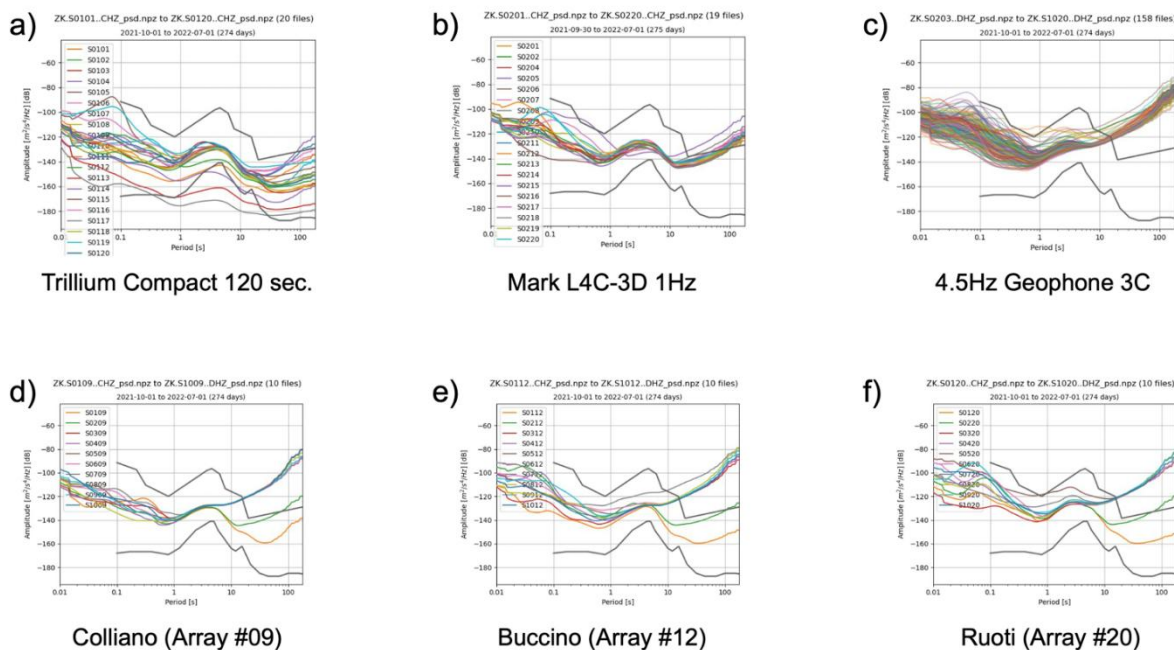
199 GIPP tools were used for data conversion from Data-Cube to standard miniseed format
200 ([https://www.gfz.de/en/section/geophysical-imaging/infrastructure/geophysical-instrument-pool-potsdam-](https://www.gfz.de/en/section/geophysical-imaging/infrastructure/geophysical-instrument-pool-potsdam-gipp/software/gipptools)
201 [gipp/software/gipptools](https://www.gfz.de/en/section/geophysical-imaging/infrastructure/geophysical-instrument-pool-potsdam-gipp/software/gipptools)), using the default setup for timing. Due to *steim2* compression, the volume of miniseed
202 data was drastically reduced to 5.2TB in the EIDA data archive, under the network code ZK.

203 Data and metadata were managed in accordance with the GIPP/GEOFON policy using SeisComP (Helmholtz
204 Centre Potsdam – GFZ German Research Centre for Geosciences and GEMPA GmbH, 2008) and other data
205 management tools. The dataset was initially embargoed, with access restricted to partners directly involved in the
206 seismic deployment. After a three-year embargo period, the data have been publicly released through the GFZ
207 EIDA node.

208 To assess the noise level at all array stations, we computed median power spectral density (PSD) curves from the
209 probability density functions (PDFs) for each channel (Figure 2). The resulting curves are shown in Figure 4. The



210 first row collects PSD curves organized per sensor, including broadband sensors (Figure 4a), 1 Hz velocimeters
 211 (Figure 4b), and 4.5 Hz geophones (Figure 4c).
 212



213
 214
 215 **Figure 4.** Average PSDs grouped by sensor types (upper panels) and arrays (lower panels).
 216

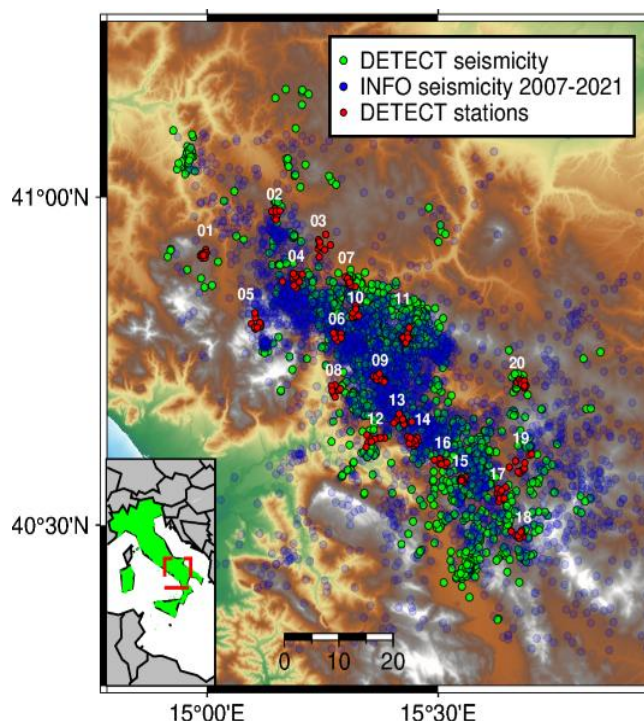
217 Below 10 Hz, the PSD curves of both the broadband and 1 Hz sensors lie well below the New High Noise Model
 218 (NHNM; Peterson, 1993). In contrast, the geophones exhibit higher noise levels, approaching the NHNM in the
 219 0.1–1 s period domain. Noise variability persists at low frequencies. Several broadband sensor curves also fall
 220 below the New Low Noise Model (NLNM) and show stable performance at periods as long as 100 s. The 1 Hz
 221 sensors clearly resolve the second microseismic peak and exhibit increased noise above 10 s, which is due to
 222 instrumental limitations. The 4.5 Hz geophones also capture the second microseismic peak, though their noise
 223 increase occurs at shorter periods. Examples of median PSD curves represented per single array are shown in the
 224 second row of Figure 4 for arrays 09 (Figure 4d), 12 (Figure 4e) and 20 (Figure 4f). In these cases, the variability
 225 of the median curves is much smaller, down to 4–5 s. Above this limit, the PSD curves diverge due to different
 226 instrumental noise at large periods (low frequencies), with curves from the geophones overcoming the reference
 227 noise curves.

228 5. Preliminary data analysis and products

229 The collected dataset of continuous waveforms offers a novel observation scale to investigate the characteristics of
 230 the seismicity in the area, shedding light on the decametric-size seismic sources for low-magnitude earthquakes.



231 A compelling example of this is provided by the enhanced catalog we compiled by applying advanced strategies.
232 For earthquake characterization, we integrated machine learning and similarity-based approaches (Scotto di Uccio
233 et al., 2023), together with the identification and relocation of earthquakes recorded during DETECT. This
234 highlights the importance of deploying dense seismic arrays for earthquake monitoring.
235



236
237
238 **Figure 5.** Earthquake epicenters occurred during the DETECT experiment (green dots), as from the seismic catalog of Scotto di Uccio et
239 al. (2026). Blue shaded dots mark the epicenters of the earthquake in the long-term INFO catalog from 2007 to the start of the array
240 deployment.
241

242 The seismic catalog was initially obtained by scanning the waveforms with the machine learning technique
243 EQTransformer (Mousavi et al., 2020), trained on the worldwide earthquake database STEAD (Mousavi et al.,
244 2019), and then refined by the template matching approach EQCorrScan (Chamberlain et al., 2018), using the
245 former catalog as the template set for the latter (Scotto di Uccio et al., 2023). Following the parameterization
246 described in Scotto di Uccio et al. (2026), the DETECT catalog contains 3.6k events, a number comparable to
247 decades of conventional monitoring, enhancing the standard catalog during the dense experiment by one order of
248 magnitude (earthquake epicenters in Figure 5).

249 We associated ~100k phase arrival times across the arrays within the catalog. Earthquake relocation revealed the
250 occurrence of microseismicity in regions with high event densities identified by the standard INFO catalog.
251 Analysis of the seismic catalog revealed a lower completeness threshold, down to -0.3, which lowered the
252 corresponding value from the long-term catalog by more than one magnitude point, as expected by the initial
253 feasibility analysis. Moreover, the b-values of the two catalogs show similar slopes in the Gutenberg–Richter
254 distribution. This indicates that the temporary deployment of dense arrays not only improves detection capability



255 but also maintains statistical consistency with long-term earthquake catalogs, effectively extending the statistical
256 characterization of seismicity to shorter time windows and lower magnitude events (Scotto di Uccio et al. 2026).
257 In this application, the seismic stations within each array were used independently, without exploiting array
258 techniques such as beamforming and back-projection. These techniques can help increase the signal-to-noise ratio
259 of the resulting waveforms and enhance the detectability of lower magnitude events. Additionally, phase arrival
260 times associated with events that occurred during the DETECT experiment can be used to train or update, using
261 transfer learning strategies, deep learning phase pickers on earthquakes with a lower magnitude range than the
262 typical population of standard and/or global datasets.

263 264 **6. Data availability**

265
266 The collected dataset is available at <https://doi:10.14470/MX7576871994> (Bindi et al. 2021), Waveform data are
267 available through the European Integrated Data Archive (EIDA) infrastructure (Strollo et al., 2021), under the
268 International Federation of Digital Seismograph Networks (FDSN) network code ZK (2021). Data are curated and
269 distributed by the GEOFON Data Center and are available under CC BY 4.0 license.

270
271 Waveform data from the ZK network can be accessed through the FDSN dataselect Web Service
272 (<https://www.fdsn.org/services>). To request specific time windows of data, a query can be constructed with
273 parameters such as network code (net), station code (sta), channel (cha), start time (starttime), and end time
274 (endtime).

275 Example, to retrieve a 3-minute time window around the event in Figure 1, including only the vertical channels of
276 the Trillium Compact 120 and the Mark L-4C-3D 1 Hz Geophone:

- 277
278 • https://geofon.gfz.de/fdsnws/dataselect/1/query?net=ZK&sta=* &cha=CHZ&starttime=2021-10-03T04:22:00&endtime=2021-10-03T04:25:00

280
281
282
283
284
285 Waveform metadata are available via standard FDSN web services and formats (<https://www.fdsn.org/services>)
286 alongside other custom services and products. Station metadata for the ZK network can be accessed through the
287 FDSN station Web Service in text format for station and channel levels, respectively:

- 288 • http://geofon.gfz.de/fdsnws/station/1/query?starttime=2021-08-15T00%3A00%3A00&endtime=2022-08-15T00%3A00%3A00&network=ZK&station=* &level=station&format=text&nodata=404
- 289
290
291 • http://geofon.gfz.de/fdsnws/station/1/query?starttime=2021-08-15T00%3A00%3A00&endtime=2022-08-15T00%3A00%3A00&network=ZK&station=* &level=channel&format=text&nodata=404



stationXML format metadata can be obtained using the following queries, respectively, for station, channel, and response levels:

- http://geofon.gfz.de/fdsnws/station/1/query?starttime=2021-08-15T00%3A00%3A00&endtime=2022-08-15T00%3A00%3A00&network=ZK&station=* &level=station&format=xml&nodata=404
- http://geofon.gfz.de/fdsnws/station/1/query?starttime=2021-08-15T00%3A00%3A00&endtime=2022-08-15T00%3A00%3A00&network=ZK&station=* &level=channel&format=xml&nodata=404
- http://geofon.gfz.de/fdsnws/station/1/query?starttime=2021-08-15T00%3A00%3A00&endtime=2022-08-15T00%3A00%3A00&network=ZK&station=* &level=response&format=xml&nodata=404

Additional data access tools include:

the interactive availability calendar view (2021-2022).

- <https://geofon.gfz.de/waveform/archive/data.php?ncode=ZK&year=2021>

the FDSN Availability web service:

- https://geofon.gfz.de/fdsnws/availability/1/query?network=ZK&station=* &start=2021-08-15T00:00:00&end=2022-08-15T00:00:00

the WFcatalog quality metrics: availability, RMS, gaps, overlaps, records, timing quality. For example, for station S0101, channel CHZ:

- <https://geofon.gfz.de/eidaws/wfcatalog/1/query?net=ZK&station=S0101&channel=CHZ&start=2021-08-15T00:00:00.000Z&end=2022-08-15T23:59:59.999Z&include=all>

the Power Spectral Density PSD (example for station S0101, channel CHZ) as for the figures included in the annexes

- https://geofon.gfz.de/eidaws/seedpsd/1/histogram?&cmmap=viridis&fontsize=12&grid=true&mean=true&noise=true&percentiles=false&&dpi=600&network=ZK&station=S0101&location=* &channel=CHZ&nodata=404&start=2021-08-15&end=2022-08-15

Finally, the seismic catalog derived from the DETECT dataset by Scotto di Uccio et al. (2026) can be accessed via Zenodo at <https://doi.org/10.5281/zenodo.15372023> (Scotto di Uccio et al., 2025) and is distributed under a Creative Commons Attribution 4.0 International license.



330 7 Conclusions

331 The DETECT experiment was a multi-institutional collaboration that promoted the concept of using micro arrays
332 in high seismic hazard regions to monitor seismicity over a short time scale. The pivotal idea behind the short-term
333 dense array deployment was to offer a novel, lower spatial scale to potentially image and track the presence of
334 crustal fluids by lowering the minimum magnitude of detectable earthquakes. Indeed, integrating small-scale
335 seismic arrays within classic seismic networks and with novel approaches for data mining allows to significantly
336 improve the detection of microseismicity, identifying in just one year the number of detected events as from decades
337 of conventional monitoring. The availability of enhanced seismic catalogs is indeed a fundamental prerequisite for
338 improving our understanding of fault mechanics. From a logistic perspective, the main challenge revealed to be the
339 scheduling and the rolling out of a well-coordinated maintenance plan over short time windows. Furthermore,
340 involving citizens in seismic experiments and monitoring activities allowed, on one hand, to speed up the siting
341 operations and increased the security of the instrumentation while, on the other hand, helped us to share knowledge
342 on seismic risk, which can contribute to raising awareness, well-being and resilience. Temporary experiments, such
343 as DETECT, can significantly help improve the knowledge about the propagation medium. Data collected during
344 the DETECT survey has the potential to provide an enriched catalog that can be exploited to derive 4D (space and
345 time) high-resolution tomographic images in velocity and attenuation to characterize variations of rock properties
346 in the fluid-filled porous medium, where micro-seismicity is diffuse and large earthquakes can nucleate. This
347 dataset could even be suitable for developing and testing ambient noise tomography repeated over time.
348 Furthermore, as that evaluation of source parameters from standard monitoring networks and surface recordings is
349 hindered by attenuation effects, that filters out the high-frequency source radiation, we believe that the dense, near-
350 fault networks recording at high sampling rates, as tested in DETECT, can help to overcome these limitations. They
351 also allow better estimation of local attenuation factors, which in turn enables a more accurate assessment of the
352 resolution limits of source parameters (Moratto et al., 2025), providing a better estimate of the epistemic
353 uncertainties affecting the source scaling relationships. Beyond the waveform dataset, the availability of the
354 enhanced catalog of Scotto di Uccio et al. (2026) substantially increases the scientific value of the dataset, providing
355 a ready-to-use resource that enables a broad range of state-of-the-art analyses without requiring users to perform
356 complex preprocessing and event characterization from scratch.

357 Regarding the monitoring infrastructure, the experimental setup of DETECT provides a useful strategy for a long-
358 term monitoring approach, where dense measurements lasting for one year are repeated every 3 to 5 years.
359 Repeating the experiment at regular time intervals allows tracking the evolution of the fault system over different
360 time scales. Thus, DETECT can be used to establish a framework for discussing the potential development of a
361 long-term project with other partners, aimed at covering the entire Italian territory with mobile seismic arrays.

362 Appendices

363 We provide as supplementary material, together with additional figures, specifically:

- 364 - Availability figures per each array (01-20, Table 2) generated with obspy-scan (Beyreuther et al., 2010)
- 365 - Probability Density Functions (PDF) all stations/components generated using
- 366 obspy.signal.spectral_estimation.PPSD (Beyreuther et al., 2010). All images are also available from
- 367 GEOFON data centre (see Data Availability section).
- 368



- 369 - Power Spectral Densities computed to generate the PDF have been averaged over the entire time span and
370 grouped in plots by array (01-20, Table 2) and by sensor type (Table 1) and resulting figures included in
371 appendix
372 - Metadata for all ZK stations as provided by the standard fdsnws-station web service (text and xml formats)
373 are also included

374 **Author contribution**

375 FSDU, AS, MP, GF, TAS, GMA, DB provided contributions to the conceptualization and finalization of the
376 article. All Authors contributed to the collection of the actual data set presented. Regarding the figures: FSDU
377 prepared Figures 1 and 5. AS prepared Figure 2, 3 and 4.

378 **Competing interest**

379 The authors declare that they have no conflict of interest.

380 **Acknowledgements**

381 We thank Karl-Heinz Jaeckel for all useful technical discussions and support during the preparation phase of the
382 experiment. The Geophysical Instrument Pool Potsdam (GIPP, <https://www.gfz.de/gipp>) provided the instruments
383 free of charge under grant number 202119 (<https://gipp.gfz.de/projects/view/754>), the GEOFON data centre
384 provided the long-term data archiving, and the GFZ financially supported the experiment with internal expedition
385 funds for logistics and the purchase of part of the batteries. Data were processed using Obspy (Beyreuther et al.,
386 2010) and figures prepared using Python, Matplotlib and Matlab.

387 We are grateful for the support of all the municipalities involved and other local authorities, local police, civil
388 protection, etc. A special mention goes to the Municipality of Colliano (SA) for hosting and organising the first
389 introductory event to involve all the other Municipalities, in particular we thank the mayor in charge during the
390 experiment, who made this possible, Adriano Goffredo, and the Councilor Giuseppe Scaglione for their
391 extraordinary commitment to support the experiment and also for liaising with other Municipalities when needed.
392 Finally, we owe a huge debt of gratitude to all the families who offered their private rooms and gardens to host and
393 look after one of our stations, and to all the helping hands during the experiment.



394 References

- 395 Adil, M., Palo, M., Zollo, A., Orefice, A., & Dell'Elce, G.: Using Repeating Microearthquakes to Infer Medium
396 Velocity Variations at Val d'Agri Area (Southern Italy). *IEEE Journal of Selected Topics in Applied Earth*
397 *Observations and Remote Sensing*, 19, 2189–2199. <https://doi.org/10.1109/JSTARS.2025.3643734>, 2025.
- 398 Adinolfi, G. M., Cesca, S., Picozzi, M., Heimann, S., and Zollo, A.: Detection of weak seismic sequences based
399 on arrival time coherence and empiric network detectability: an application at a near fault observatory,
400 *Geophysical Journal International*, 218, 2054–2065, <https://doi.org/10.1093/gji/ggz248>, 2019.
- 401 Amoroso, O., Ascione, A., Mazzoli, S., Virieux, J., and Zollo, A.: Seismic imaging of a fluid storage in the
402 actively extending Apennine mountain belt, southern Italy, *Geophysical Research Letters*, 41, 3802–3809,
403 <https://doi.org/10.1002/2014GL060070>, 2014.
- 404 Bello, S., de Nardis, R., Scarpa, R., Brozzetti, F., Cirillo, D., Ferrarini, F., di Lieto, B., Arrowsmith, R. J., and
405 Lavecchia, G.: Fault Pattern and Seismotectonic Style of the Campania – Lucania 1980 Earthquake (Mw 6.9,
406 Southern Italy): New Multidisciplinary Constraints, *Front. Earth Sci.*, 8,
407 <https://doi.org/10.3389/feart.2020.608063>, 2021.
- 408 Ben-Zion, Y., Vernon, F. L., Ozakin, Y., Zigone, D., Ross, Z. E., Meng, H., White, M., Reyes, J., Hollis, D., and
409 Barklage, M.: Basic data features and results from a spatially dense seismic array on the San Jacinto fault zone,
410 *Geophysical Journal International*, 202, 370–380, <https://doi.org/10.1093/gji/ggv142>, 2015.
- 411 Bernard, P. and Zollo, A.: The Irpinia (Italy) 1980 earthquake: Detailed analysis of a complex normal faulting,
412 *Journal of Geophysical Research: Solid Earth*, 94, 1631–1647, <https://doi.org/10.1029/JB094iB02p01631>, 1989.
- 413 Beyreuther, M., Barsch, R., Krischer, L., Megies, T., Behr, Y., and Wassermann, J.: ObsPy: A Python Toolbox
414 for Seismology, *Seismological Research Letters*, 81, 530–533, <https://doi.org/10.1785/gssrl.81.3.530>, 2010.
- 415 Bindi, D., Cotton, F., Picozzi, M., and Zollo, A.: The Irpinia seismic Array, ~1T,
416 <https://doi.org/10.14470/MX7576871994>, 2021.
- 417 Caracausi, A., Buttitta, D., Picozzi, M., Paternoster, M., and Stabile, T. A.: Earthquakes control the impulsive
418 nature of crustal helium degassing to the atmosphere, *Commun Earth Environ*, 3, 224,
419 <https://doi.org/10.1038/s43247-022-00549-9>, 2022.
- 420 Chamberlain, C. J., Hopp, C. J., Boese, C. M., Warren-Smith, E., Chambers, D., Chu, S. X., Michailos, K., and
421 Townend, J.: EQcorrscan: Repeating and Near-Repeating Earthquake Detection and Analysis in Python,
422 *Seismological Research Letters*, 89, 173–181, <https://doi.org/10.1785/0220170151>, 2018.
- 423 Chiaraluce, L., Festa, G., Bernard, P., Caracausi, A., Carluccio, I., Clinton, J., ... and Sokos, E. . The Near Fault
424 Observatory community in Europe: a new resource for faulting and hazard studies. *Array*, 65(3), DM316, 2022.
425



- 426 Chiodini, G., Cardellini, C., Amato, A., Boschi, E., Caliro, S., Frondini, F., and Ventura, G.: Carbon dioxide
427 Earth degassing and seismogenesis in central and southern Italy, *Geophysical Research Letters*, 31,
428 <https://doi.org/10.1029/2004GL019480>, 2004.
- 429 D’Agostino, N., Silverii, F., Amoroso, O., Convertito, V., Fiorillo, F., Ventafriidda, G., and Zollo, A.: Crustal
430 Deformation and Seismicity Modulated by Groundwater Recharge of Karst Aquifers, *Geophysical Research*
431 *Letters*, 45, 12,253-12,262, <https://doi.org/10.1029/2018GL079794>, 2018.
- 432 De Landro, G., Picozzi, M., Russo, G., Adinolfi, G. M., and Zollo, A.: Seismic networks layout optimization for
433 a high-resolution monitoring of induced micro-seismicity, *J Seismol*, 24, 953–966,
434 <https://doi.org/10.1007/s10950-019-09880-9>, 2020.
- 435 De Landro, G., Amoroso, O., Russo, G., D’Agostino, N., Esposito, R., Emolo, A., and Zollo, A.: Decade-long
436 monitoring of seismic velocity changes at the Irpinia fault system (southern Italy) reveals pore pressure
437 pulsations, *Sci Rep*, 12, 1247, <https://doi.org/10.1038/s41598-022-05365-x>, 2022.
- 438 DISS Working Group. Database of Individual Seismogenic Sources (DISS), Version 3.3.1: A compilation of
439 potential sources for earthquakes larger than M 5.5 in Italy and surrounding areas. Istituto Nazionale di Geofisica
440 e Vulcanologia (INGV). <https://doi.org/10.13127/diss3.3.1>, 2025.
- 441 Di Luccio, F., Ventura, G., Di Giovambattista, R., Piscini, A., and Cinti, F. R.: Normal faults and thrusts
442 reactivated by deep fluids: The 6 April 2009 M 6.3 L’Aquila earthquake, central Italy, *Journal of Geophysical*
443 *Research: Solid Earth*, 115, <https://doi.org/10.1029/2009JB007190>, 2010.
- 444 Festa, G., Adinolfi, G. M., Caruso, A., Colombelli, S., De Landro, G., Elia, L., Emolo, A., Picozzi, M., Scala, A.,
445 Carotenuto, F., Gammaldi, S., Iaccarino, A. G., Nazeri, S., Riccio, R., Russo, G., Tarantino, S., and Zollo, A.:
446 Insights into Mechanical Properties of the 1980 Irpinia Fault System from the Analysis of a Seismic Sequence,
447 *Geosciences*, 11, 28, <https://doi.org/10.3390/geosciences11010028>, 2021.
- 448 Gradon, C., Roux, P., Moreau, L., Lecointre, A., and Ben Zion, Y.: Characterization with dense array data of
449 seismic sources in the shallow part of the San Jacinto fault zone, *Geophysical Journal International*, 224, 1133–
450 1140, <https://doi.org/10.1093/gji/ggaa411>, 2020.
- 451 Heit, B., Cristiano, L., Haberland, C., Tilmann, F., Pesaresi, D., Jia, Y., ... and Weber, M. : The SWATH-D
452 seismological network in the Eastern Alps. *Seismological Society of America*, 92(3), 1592-1609, 2021.
453
- 454 Helmholtz-Centre Potsdam-GFZ German Research Centre For Geosciences and GEMPA GmbH: The SeisComp
455 seismological software package, , <https://doi.org/10.5880/GFZ.2.4.2020.003>, 2008.
- 456 Iannaccone, G., Zollo, A., Elia, L., Convertito, V., Satriano, C., Martino, C., ... and Emolo, A: A prototype
457 system for earthquake early-warning and alert management in southern Italy. *Bulletin of Earthquake Engineering*,
458 8(5), 1105-1129, 2010.
459



- 460 Improta, L., De Gori, P., and Chiarabba, C.: New insights into crustal structure, Cenozoic magmatism, CO₂
461 degassing, and seismogenesis in the southern Apennines and Irpinia region from local earthquake tomography,
462 *Journal of Geophysical Research: Solid Earth*, 119, 8283–8311, <https://doi.org/10.1002/2013JB010890>, 2014.
- 463 Moratto, L., Panebianco, S., Satriano, C., Stabile, T. A., and Priolo, E.: Using ambient noise k₀ estimation to
464 improve microearthquake source parameters assessment in the High Agri Valley, *Geophysical Journal
465 International*, 242(2), ggaf191, <https://doi.org/10.1093/gji/ggaf191>, 2025.
- 466 Mousavi, S. M., Sheng, Y., Zhu, W., and Beroza, G. C.: STanford EArthquake Dataset (STEAD): A Global Data
467 Set of Seismic Signals for AI, *IEEE Access*, 7, 179464–179476, <https://doi.org/10.1109/ACCESS.2019.2947848>,
468 2019.
- 469 Mousavi, S. M., Ellsworth, W. L., Zhu, W., Chuang, L. Y., and Beroza, G. C.: Earthquake transformer—an
470 attentive deep-learning model for simultaneous earthquake detection and phase picking, *Nat Commun*, 11, 3952,
471 <https://doi.org/10.1038/s41467-020-17591-w>, 2020.
- 472 Palo, M., Picozzi, M., De Landro, G., and Zollo, A.: Microseismicity clustering and mechanic properties reveal
473 fault segmentation in southern Italy, *Tectonophysics*, 856, 229849, <https://doi.org/10.1016/j.tecto.2023.229849>,
474 2023.
- 475 Panebianco, S., Satriano, C., Vivone, G., Picozzi, M., Strollo, A., and Stabile, T. A.: Automated Detection and
476 Machine Learning-Based Classification of Seismic Tremors Associated With a Non-Volcanic Gas Emission
477 (Mefite d’Ansanto, Southern Italy), *Geochemistry, Geophysics, Geosystems*, 25, e2023GC011286,
478 <https://doi.org/10.1029/2023GC011286>, 2024.
- 479 Peterson, J.: Observations and modeling of seismic background noise, *US Geol. Surv. Open-File Rept.* 93, 322,
480 95, 1993.
- 481 Picozzi, M., Milkereit, C., Fleming, K., Çakti, E., and Zschau, J.: A generalized zero-lag cross-correlation
482 approach for Rapid Earthquake Localization (REL): the example of the Istanbul Megacity Rapid Response
483 System, *J Seismol*, 15, 557–578, <https://doi.org/10.1007/s10950-011-9232-0>, 2011.
- 484 Picozzi, M., Bindi, D., Zollo, A., Festa, G., and Spallarossa, D.: Detecting long-lasting transients of earthquake
485 activity on a fault system by monitoring apparent stress, ground motion and clustering, *Sci Rep*, 9, 16268,
486 <https://doi.org/10.1038/s41598-019-52756-8>, 2019.
- 487 Picozzi, M., Spallarossa, D., Iaccarino, A. G., and Bindi, D.: Temporal Evolution of Radiated Energy to Seismic
488 Moment Scaling During the Preparatory Phase of the Mw 6.1, 2009 L’Aquila Earthquake (Italy), *Geophysical
489 Research Letters*, 49, e2021GL097382, <https://doi.org/10.1029/2021GL097382>, 2022a.
- 490 Picozzi, M., Bindi, D., Festa, G., Cotton, F., Scala, A., and D’Agostino, N.: Spatiotemporal Evolution of
491 Microseismicity Seismic Source Properties at the Irpinia Near-Fault Observatory, Southern Italy, *Bulletin of the
492 Seismological Society of America*, 112, 226–242, <https://doi.org/10.1785/0120210064>, 2022b.



- 493 Picozzi, M., Cotton, F., Bindi, D., Emolo, A., Maria Adinolfi, G., Spallarossa, D., and Zollo, A.: Spatiotemporal
494 Evolution of Ground-Motion Intensity at the Irpinia Near-Fault Observatory, Southern Italy, *Bulletin of the*
495 *Seismological Society of America*, 112, 243–261, <https://doi.org/10.1785/0120210153>, 2022c
- 496 Rost, S. and Thomas, C.: Improving Seismic Resolution Through Array Processing Techniques, *Surv Geophys*,
497 30, 271–299, <https://doi.org/10.1007/s10712-009-9070-6>, 2009.
- 498 Rovida A., Locati M., Camassi R., Lolli B., Gasperini P.: The Italian earthquake catalogue CPTI15. *Bulletin of*
499 *Earthquake Engineering*, 18(7), 2953–2984. <https://doi.org/10.1007/s10518-020-00818-y>, 2020.
500
- 501 Scala, A., Adinolfi, G. M., Picozzi, M., Scotto Di Uccio, F., Festa, G., De Landro, G., Priolo, E., Parolai, S.,
502 Riccio, R., and Romanelli, M.: Monitoring the Microseismicity through a Dense Seismic Array and a Similarity
503 Search Detection Technique: Application to the Seismic Monitoring of Collalto Gas-Storage, North Italy,
504 *Energies*, 15, 3504, <https://doi.org/10.3390/en15103504>, 2022.
- 505 Scotto di Uccio, F., Scala, A., Festa, G., Picozzi, M., and Beroza, G. C.: Comparing and integrating artificial
506 intelligence and similarity search detection techniques: application to seismic sequences in Southern Italy,
507 *Geophysical Journal International*, 233, 861–874, <https://doi.org/10.1093/gji/ggac487>, 2023.
- 508 Scotto di Uccio, F., Michele, M., Strumia, C., Supino, M., Beroza, G. C., Chiaraluca, L., D’Agostino, N., and
509 Festa, G.: Characterization and Evolution of Seismic Sequences in the Normal Fault Environment of the Southern
510 Apennines, *Journal of Geophysical Research: Solid Earth*, 129, e2023JB028644,
511 <https://doi.org/10.1029/2023JB028644>, 2024.
- 512 Scotto di Uccio, F., Muzellec, T., Scala, A., De Landro, G., Camanni, G., Carotenuto, F., Elia, L., Picozzi, M.,
513 Zollo, A., Strumia, C., Beroza, G., and Festa, G. (2025). Enhanced seismic catalog for the seismicity observed
514 during the DETECT experiment, Southern Italy [Data set]. Zenodo. <https://doi.org/10.5281/zenodo.15372023>
515
- 516 Scotto di Uccio, F., Muzellec, T., Scala, A., De Landro, G., Camanni, G., Carotenuto, F., Elia, L., Picozzi, M.,
517 Zollo, A., Strumia, C., Beroza, G. C., and Festa, G.: Enhancing the resolution of microseismicity through dense
518 array monitoring in complex extensional settings. *Scientific Reports*, 16, 5639, <https://doi.org/10.1038/s41598-026-35586-3>, 2026.
519
- 520
- 521 Stabile, T. A., Satriano, C., Orefice, A., Festa, G., and Zollo, A.: Anatomy of a microearthquake sequence on an
522 active normal fault, *Sci Rep*, 2, 410, <https://doi.org/10.1038/srep00410>, 2012.
- 523 Stabile, T. A., Vlček, J., Wcisło, M., and Serlenga, V.: Analysis of the 2016–2018 fluid-injection induced
524 seismicity in the High Agri Valley (southern Italy) from improved detections using template matching, *Sci Rep*,
525 11(1), 20630, <https://doi.org/10.1038/s41598-02100047-6>, 2021.
- 526 Strollo, A., Cambaz, D., Clinton, J., Danecek, P., Evangelidis, C. P., Marmureanu, A., ... and Triantafyllis, N. .
527 EIDA: The European integrated data archive and service infrastructure within ORFEUS. *Seismological Society*
528 *of America*, 92(3), 1788–1795. 2021
529



530 Tarantino, S., Poli, P., D'Agostino, N., Vassallo, M., Festa, G., Ventafridda, G., and Zollo, A.: Non-linear
531 elasticity, earthquake triggering and seasonal hydrological forcing along the Irpinia fault, Southern Italy, Nat
532 Commun, 15, 9821, <https://doi.org/10.1038/s41467-024-54094-4>, 2024.